

## UC Davis IDAV Publications

### Title

An Ocularist's Approach to Human Iris Synthesis

### Permalink

<https://escholarship.org/uc/item/8d88d3qc>

### Journal

IEEE Computer Graphics and Applications, 23

### Authors

Lefohn, Aaron  
Caruso, Richard  
Reinhard, Erik  
[et al.](#)

### Publication Date

2003

Peer reviewed

# An Ocularist's Approach to Human Iris Synthesis

Aaron Lefohn  
University of Utah

Richard Caruso  
Eye Prosthetics of Utah, Inc.

Erik Reinhard  
University of Central Florida

Brian Budge  
University of Utah

Peter Shirley  
University of Utah

## Abstract

Human irises gain their appearance from a layered and highly complex structure that is difficult to model and render with conventional techniques. We present an approach that uses domain knowledge from the field of ocular prosthetics. In that field, ocularists create an artificial iris by painting many simple semi-transparent layers. We translate this methodology into a simple and effective toolkit which can be used to create and render realistic looking irises.

**keywords:**Color, Shading, Rendering, Iris, Eye, Texture

## 1 Introduction

While recent advances in modeling and rendering have generally facilitated the production of realistic imagery, certain specialized modeling and rendering tasks remain difficult. One such challenge is presented by the human eye, which exhibits intricate detail in the iris that is complex enough to serve as an alternative to fingerprints for personal identification [Daugman 1993].

One of the biggest challenges in realistic rendering is knowing what features of a model are important for realism, and what can be ignored. This issue is particularly vexing in synthesis because the anatomical literature is incomplete, and the salient aspects of iris appearance have not been studied. However, we have a particularly fortunate situation in iris synthesis: artificial eye makers (ocularists) have developed a procedure for physical iris synthesis that results in eyes with all the important appearance characteristics of real eyes. Their procedure has been refined over decades, and the most complete validation one could ask for is provided by the performance of their products in the real world.

In this paper, we present an approach that enables users other than trained ocularists to create a realistic looking human eye, paying particular attention to the iris. We draw from domain knowledge provided by ocularists to provide a toolkit that allows the composition of a human iris by layering semi-transparent textures. These textures look decidedly painted and unrealistic. The composited result, however, provides a sense of depth to the iris and takes on a level of realism that we believe has not been achieved before.

Previous work on rendering eyes has concentrated predominantly on producing geometry for facial animation [Parke and Waters 1996] or for medical applications [Sagar et al. 1994]. Some work has focused on accurately modeling the cornea [Halstead et al. 1996; Barsky et al. 1999]. In contrast, the goal of this work is to allow the easy creation of realistic looking irises for both the ocular prosthetics and entertainment industries.

In Section 2 we introduce the terminology for describing the anatomy of human eyes and irises, both in terms of medical applications and from the point of view of ocularists. Our contribution to the field of graphics includes the translation of the way ocularists work to a simple, semi-automated method of modeling and rendering human irises. This method is presented in Section 3, while our results are discussed in Section 4. Conclusions are drawn in Section 5.

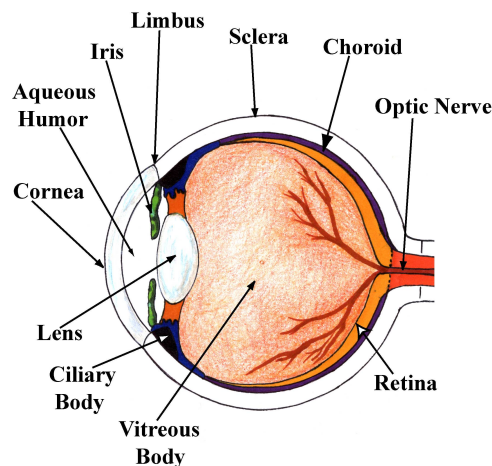


Figure 1: *The human eye.* Drawing by Karen Lefohn. Used with permission.

## 2 The Human Eye

### 2.1 Overview

The human eye is an organ designed for photo-reception; i.e. converting light energy to nerve action potentials. These action potentials are subsequently relayed to the optic nerve and the brain, where further processing occurs, resulting in conscious vision. All structures in the eye are subservient to this physiological process [Forrester et al. 2001].

The largest structure of the eye is the sclera (Figure 1), which is approximately spherical with a radius of around 11.5 mm. The cornea sits somewhat in front of this structure and has a radius of 7.8 mm. The sclera takes around  $5/6^{\text{th}}$  of the circumference of the eye, while the cornea is responsible for the other  $1/6^{\text{th}}$ . The transition zone between sclera and cornea is called the limbus and has a fuzzy appearance. The eye contains three basic layers: the fibrous (corneo-scleral) coat, the uvea or uveal tract (choroid, ciliary body and iris) and the neural layer (retina). These coats surround the contents of the eye, which are the lens, the aqueous humor and the vitreous body [Forrester et al. 2001]. The cornea, with an index of refraction of 1.376, is responsible for most of the refractive power of the eye. After the cornea, light passes through the aqueous humor (index of refraction 1.336), the lens (index of refraction ranges from 1.386 in the outer layers to 1.406 at the center) and the vitreous body (index of refraction 1.337) before it reaches the retina [Hecht 1987].

### 2.2 The Iris

The iris is part of the uveal tract, which also includes the ciliary body and the choroid. Its function is to control the amount of light

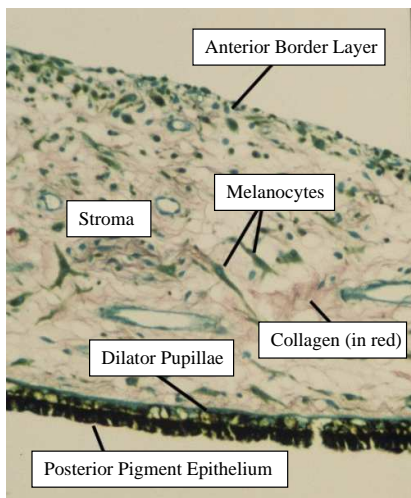


Figure 2: Cross section of the iris (adapted from [Forrester et al. 2001]). Used with permission.

that reaches the retina. Due to its heavy pigmentation, light can only pass through the iris via the pupil, which contracts and dilates according to the amount of available light. Irises are pigmented with melanin and lipofuscin (also known as lipochrome) [Sarna and Sealy 1984; Delori and Pflibsen 1988; Clancy et al. 2000]. Iris dimensions vary slightly between individuals, but on average it is 12 mm in diameter [Forrester et al. 2001]. Its shape is conical with the pupillary margin located more anteriorly than the root. The anterior surface is divided into the ciliary zone and the pupil zone by a thickened region called the collarette. There are four layers in the iris: the anterior border layer, the stroma, the dilator pupillae muscle and the posterior pigment epithelium (Figure 2).

The anterior border layer consists mainly of a dense collection of fibroblasts and melanocytes. It is deficient in some areas, causing crypts, and heavily pigmented in other areas, which appear as naevi. The stroma is a layer of loosely connected tissue containing collagen, melanocytes, mast cells and macrophages. Many of the macrophages and melanocytes are heavily pigmented. The dilator pupillae muscle is responsible for dilation (mydriasis), which normally occurs in dark conditions. Its cells are normally lightly pigmented. The posterior pigment epithelium appears black macroscopically and prevents light from leaking through the iris. Finally, the sphincter pupillae muscle is concentric and lies near the pupillary margin. It is responsible for contraction (miosis).

These layers together determine eye color through a combination of scattering effects and pigmentation. Brown eyes are due to heavy pigmentation of the anterior border layer with eumelanin. Blue eyes are due to Rayleigh scattering of light in the stroma [Keating 1988]. For less translucent eyes, the resulting color is grey. Hazel eyes are caused by a combination of melanin in the anterior border layer and scattering. Yellow specks or patches may occur due to the presence of lipofuscin.

A model of the iris should capture the shape of the iris as well as its patterns and colors. The general conical shape can be captured by the surface of revolution technique described in Section 3. The patterns that are formed by crypts and naevi could be produced procedurally or could be captured using image based techniques. Unfortunately, sufficiently detailed anatomical descriptions of the iris are not available in the medical literature. Moreover, image based techniques would involve specialized equipment of the kind normally found only in eye hospitals. By using the domain knowledge of ocular prosthetics, we are able to produce a practical method to model and render irises.

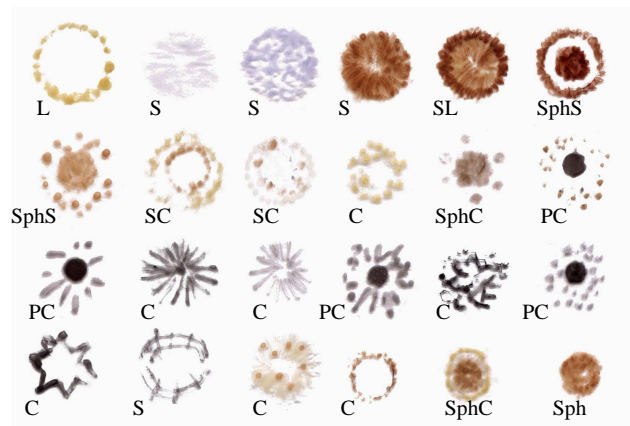


Figure 3: Example layers containing stroma (S), collarette (C), limbus (L), pupil (P) and sphincter muscle (Sph) components. Layers containing multiple components are labeled with multiple letters.

Although each ocularist has his/her own style of painting and working methodology, general guidelines can be provided. Ocularists paint eyes using between 30 to 70 different layers of paint, with layers of clear coat between them. The first layer, called the base layer, contains the most dominant colors found in the eye, and is painted on a black opaque iris button (Figure 5). For a grey or blue eye, this layer tends to contain a fair amount of white. For brown eyes, this color may be darker. Each subsequent layer consists of one or two of the following components (see also Figure 3):

**Stroma** This component covers nearly all of the iris area and consists of a number of well defined dots, smeared dots or radial smears.

**Collarette** The collarette component is confined to the inner half of the iris and contains either radial spokes or dots (the latter being either well-defined or smeared).

**Sphincter** The sphincter component is usually a colored ring, lying close to the pupil.

**Limbus** The border between the cornea and the sclera is usually made fuzzy and darker than the rest of the eye. Although not completely anatomically correct, this component is normally painted as part of the iris.

**Pupil** The pupil is normally painted in multiple layers and appears simply as a black dot.

The amount of detail visible in the iris varies from person to person and is correlated to eye color. Brown eyes tend to have less detail and have a smudged or smeared appearance, whereas lighter eye colors show more detail. Ocularists distinguish between three different types of eye with the descriptive names: smeared, dit-dot and detail. While every eye will contain each of the components listed above, a smeared eye will predominantly consist of smeared versions of the stroma, collarette and sphincter components. Dit-dot and detail eyes on the other hand, contain more well-defined painted layers.

The number of different paint colors is typically less than 10. An example of the base colors derived from these paints used to produce prosthetic eyes is given in Figure 4. These base colors are then pairwise mixed to form the prevailing color for each layer.



Figure 4: Paint mixtures that are usually pairwise mixed to form the color for each layer.



Figure 5: Typical base layers for blue eyes (first three), a green eye and a brown eye.

### 3 Method

Our aim is to provide a practical method that allows users to create a believable rendition of a human eye, and in particular a human iris. The approach is based on a small set of simple techniques to create 3D geometry, to create realistic iris patterns and colorations, and to render the result. Each of these stages is detailed in the following sections.

#### 3.1 Eye Geometry

Although the human eye is slightly asymmetrical and the pupil is placed slightly off-center [Hogan et al. 1971], for most practical purposes the human eye can be thought of as symmetrical with respect to the line of sight.

In renderers that can directly render constructive solid geometry (CSG) models, the geometry of the human eye may be approximated by two spheres, as shown in Figure 6. However, many renderers do not directly support CSG, and we therefore present a convenient alternative. All parts of the eye can be modeled with primitives called “frustums of right circular cones”, i.e. megaphone-shaped objects, which from here on we will call cones. This primitive was chosen over more powerful modeling primitives such as splines because generating the 3D model from a 2D drawing using cones is trivial, as explained next. Simpler primitives such as triangles or polygons would also present unnecessary challenges in the modeling stage.

To capture the shape of the sclera, iris and cornea, we start with a 2D cross section which is to scale, such as figure 6 or 7. A cone is specified by two 3D position vectors representing the center of the cone’s top and bottom. Associated with these two centers are two radii. The center coordinates are found by measuring in the figure their distances to the origin of the model, which we arbitrarily choose to be as indicated in Figure 7. The radii are measured similarly. The surface being modeled can be made arbitrarily smooth by choosing a smaller cone height. These piecewise-linear surfaces of revolution are used to model the entire eye.

This approach emphasizes ease of modeling, but creates models that are somewhat inefficient to render. The cones have a wide base, but are not very high, leading to an awkward shape to render efficiently with currently popular spatial subdivision methods. For example, for a grid the number of voxels along the z-axis could adapt to the number of cones. However, a small number of voxels

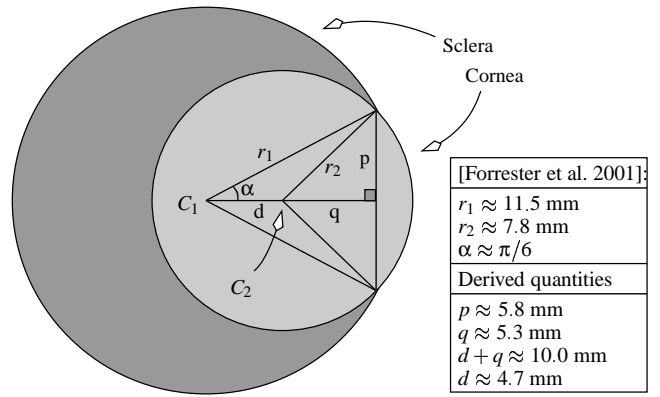


Figure 6: Cross section of a human eye, drawn to scale. The geometry of a human eye can be approximated by two spheres with radii of  $r_1 \approx 11.5$  mm. and  $r_2 \approx 7.8$  mm. The centers  $C_1$  and  $C_2$  of these spheres should be approximately  $d \approx 4.7$  mm. apart.

in the x and y directions would lead to too many intersection tests, whereas a large number of voxels would lead to many empty cells, making ray traversal too expensive.

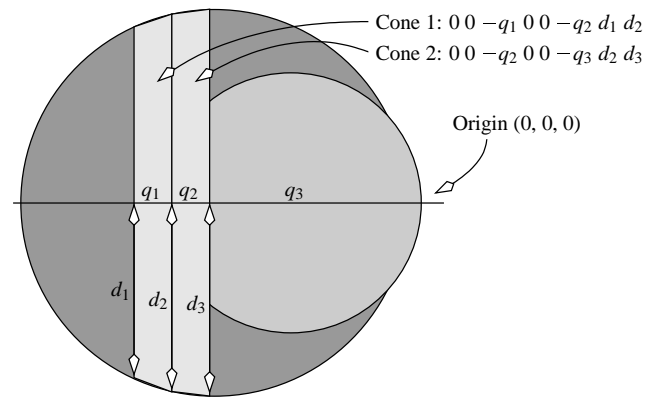


Figure 7: Creating a 3D model consisting of cones by tracing coordinates. Distances  $q_i$  are measured with respect to the origin, and radii  $d_i$  are measured from the center axis. Note that this figure has been drawn to scale.

We limit ourselves to modeling the sclera, iris and cornea, because other parts of the eye, such as the lens, the vitreous body and the retina, only contribute to the rendered results in very rare and specific cases. An example which we are currently not able to recreate is light scattering off the back of the retina. The aqueous humor is not modeled because its index of refraction is very similar to that of the cornea. Hence, its contribution to the rendered result is small. Ocularists also make this assumption when building an ocular prosthesis.

#### 3.2 Iris Synthesis

The iris is one of the most distinguishing features of the human eye. We model its geometry with a number of closely stacked cones representing the layers that an ocularist would paint. Because an ocularist would alternate layers of paint with layers of varnish, the cones are placed close together, but far enough apart to avoid numerical instabilities. The cones are texture-mapped with semi-transparent textures, such as those in Figure 3, with the exception

of the base layer which is opaque and is texture-mapped with textures similar to those in Figure 5.

The semi-transparent layers are scanned using a conventional flat-bed scanner and the amount of transparency for each texel is inferred from these scans by converting them to gray-scale and then inverting the gray values, resulting in an opacity map for each layer. The opacity value can then be interpreted as paint density. This works under the empirical observation that transmission and reflection are similar for the paints we use.

Given the limited number of base colors used by ophthalmologists, and the fact that for each layer only two of these colors are mixed to produce the dominant color for that layer, it is possible to select a single color for each of the layers by interpolating between two paint colors, which we perform in HSL space. There are no specific rules as to which two colors (Figure 4) can be mixed.

After the base layer is selected, a number of semi-transparent layers are overlaid. The patterns are selected from Figure 3 and a single color is assigned to the transparency map. The choice of which patterns to apply and in which order is essentially free, although ophthalmologists tend to go back and forth between stroma, sphincter, collarette, limbus and pupil layers. The repeated application of high frequency, fairly opaque layers and more transparent, cloudy layers contributes significantly to the appearance of depth in the resulting model. Note that in our model, the pupil is defined implicitly by the hole in the center of the iris cones, so the painted pupil is not visible.

### 3.3 Rendering

For rendering the resulting model, we use a ray tracer which is able to render cones with transparent and opaque textures, as well as dielectric and glossy materials. The painted layers are applied to the iris cones using a semi-opaque paint model. In this model, a ray incident on a painted layer returns a color computed with

$$R = (1 - \alpha)T + \alpha CL \quad (1)$$

In this equation,  $\alpha$  is the opacity value read for a particular intersection point from the opacity map,  $T$  is the result returned from shooting a ray in the transmitted direction (index of refraction is 1.0 for layers),  $C$  is the paint color and  $L$  is the result of shooting a ray towards each light source. Shadow rays that intersect a semi-transparent texture are attenuated by

$$L' = (1 - \alpha)CL, \quad (2)$$

with  $L'$  being the attenuated color. Note that shadow rays are attenuated by the color of each layer through which they pass. This model does not include Rayleigh scattering, because we are simulating eye prostheses, not real human eyes.

Just as an ophthalmologist paints the fuzzy appearance of the limbus onto the iris, we have blended the iris into the sclera by applying an opacity map to a small cone that sits just above the top-most iris layer. The opacity map blends from completely transparent, at its inner-most point, to completely opaque as it meets the sclera. A similar technique is used to soften the appearance of the pupillary margin. To enhance the visual richness of the images, we added environment maps for both blood vessels and area light sources.

## 4 Results

Our method is capable of creating patterns and colors that match existing human irises. We show results for three eye groups: brown, blue and green. For the green eye, a matched ocular prosthesis was created. Figure 8 shows this prosthesis alongside a photograph of the same eye and a rendering created with our method. Note that

the match between the real eye and the rendered eye is close, but not identical. The same is true for the prosthetic eye. Thus, our method produces results that are of similar quality as those obtained by ophthalmologists.

Our method mimics the ophthalmologist's approach by adding one layer at a time to the model and rendering an intermediate result. This allows the incremental creation of an iris using single layers taken from our standard library of textures, although additional layers could be easily painted in standard paint programs. An example of the progression of work that led to the rendering of Figure 8 is given in Figure 9. Further examples of a rendered brown eye with 12 layers and a blue eye with 50 layers are given in Figure 10.

## 5 Discussion

We have presented a simple and effective method to create irises using ideas taken from the field of ocular prosthetics. The results obtained with our method are of similar quality to those obtained by ophthalmologists. The method will be useful in applications ranging from entertainment to ocular prosthetics. For ophthalmologists our method would provide a valuable additional pre-visualization tool, allowing layers of "paint" to be removed or altered at any time during the process. Currently, an ophthalmologist paints an eye using small and conservative steps. Our pre-visualization tool would allow an ophthalmologist to create and alter a new iris on the computer before committing his work to paint as well as showing the patient a digital prototype of the prosthesis.

## 6 Acknowledgements

The authors would like to thank Paula Morris and Professor Robert Marc at the Moran Eye Institute for sharing their time and invaluable knowledge with us. We would also like to thank Kristin Potter and Raelynn Potts for patiently allowing us to photograph their eyes. In addition, we would like to thank Karen Lefohn for providing figure 1 and Professor Paul McMenamin at the University of Western Australia for allowing us to use figure 2.

## References

- BARSKY, B., CHU, L., AND KLEIN, S. 1999. Cylindrical coordinate representations for modeling surfaces of the cornea and contact lenses. In *Proceedings of the International Conference on Shape Modeling and Applications (SMI-99)*, IEEE Computer Society, Los Alamitos, CA, B. Werner, Ed., 98–115.
- CLANCY, C., KROGMEIER, J., PAWLAK, A., ROZANOWSKA, M., SARNA, T., DUNN, R., AND SIMON, J. 2000. Atomic force microscopy and near-field scanning optical microscopy measurements of single human retinal lipofuscin granules. *J. Phys. Chem. B* 104, 12098–12102.
- DAUGMAN, J. 1993. High confidence visual recognition of persons by a test of statistical independence. *IEEE Transactions on Pattern Analysis and Machine Intelligence* 15, 11, 1148–1161.
- DELORI, F., AND PFLIBSEN, K. 1988. Spectral reflectance of the human ocular fundus. *Applied Optics* 28, 6, 1061–1077.
- FORRESTER, J., DICK, A., MCMENAMIN, P., AND LEE, W. 2001. *The eye: basic sciences in practice*. W B Saunders, London.
- HALSTEAD, M., BARSKY, B., KLEIN, S., AND MANDELL, R. 1996. Reconstructing curved surfaces from specular reflection



Figure 8: A green eye, a rendered eye using 30 textured layers, and its matched ocular prosthesis.



Figure 9: A compositing progression for the creation of the rendered green eye shown in Figure 8. The first image shows the base layer, and every subsequent image has 10 transparent layers added. The right image shows all layers.



Figure 10: A blue and a brown eye and their matched renderings.

- patterns using spline surface fitting of normals. In *SIGGRAPH 96 Conference Proceedings*, Addison Wesley, H. Rushmeier, Ed., Annual Conference Series, ACM SIGGRAPH, 335–342. held in New Orleans, Louisiana, 04–09 August 1996.
- HECHT, E. 1987. *Optics*, 2nd ed. Addison-Wesley, Reading MA.
- HOGAN, M., ALVARADO, J., AND WEDDELL, J. 1971. *Histology of the Human Eye*. W B Saunders, Philadelphia.
- KEATING, M. 1988. *Geometric, Physical, and Visual Optics*. Butterworths, Boston.
- PARKE, F., AND WATERS, K. 1996. *Computer Facial Animation*. A K Peters.
- SAGAR, M., BULLIVANT, D., MALLINSON, G., HUNTER, P., AND HUNTER, I. 1994. A virtual environment and model of the eye for surgical simulation. In *Proceedings of SIGGRAPH '94 (Orlando, Florida, July 24–29, 1994)*, ACM Press, A. Glassner, Ed., Computer Graphics Proceedings, Annual Conference Series, ACM SIGGRAPH, 205–213. ISBN 0-89791-667-0.
- SARNA, T., AND SEALY, R. 1984. Free radicals from eumelanins: Quantum yields and wavelength dependence. *Archives of Biochemistry and Biophysics* 232, 2, 574–578.